1-1-1996

Simulation of slow variable-angle spinning NMR spectra. Application to 13C bonded to N

B H. Suits
Michigan Technological University, suits@mtu.edu

J. Sepa
Michigan Technological University

David Wnite
University of Pennsylvania

Recommended Citation

Suits, B. H., Sepa, J., & Wnite, D. (1996). Simulation of slow variable-angle spinning NMR spectra. Application to 13C bonded to N. *Journal of Magnetic Resonance - Series A, 120*(1), 88-96. http://doi.org/10.1006/jmra.1996.0102
Retrieved from: https://digitalcommons.mtu.edu/michigantech-p/3975

Follow this and additional works at: https://digitalcommons.mtu.edu/michigantech-p

 Part of the Physics Commons

JOURNAL OF MAGNETIC RESONANCE, Series A **120,** 88–96 (1996)
ARTICLE NO. 0102

Simulation of Slow Variable-Angle Spinning NMR Spectra. Application to ^{13}C Bonded to N

B. H. SUITS,* J. ŠEPA,† AND DAVID WHITE†

*Physics Department, Michigan Technological University, Houghton, Michigan 49931; and †Department of Chemistry, University of Pennsylvania, Philadelphia, Pennsylvania 19104

Received January 8, 1996; revised February 16, 1996

Simulations of NMR spectra for spin-$\frac{1}{2}$ nuclei in rigid solids spun at relatively slow speeds and at angles other than the magic angle are presented. Particular emphasis is on the case where ^{13}C is bonded to a quadrupolar nucleus such as ^{14}N. The feasibility of quantitatively extracting the chemical-shift tensor, bond lengths through the dipolar interaction, and the electric-field gradient of the neighboring nucleus from a single (1-D) spectrum is demonstrated. The sensitivity of the observed changes in the spectra to changes in the physical and experimental parameters is discussed and illustrated using nitrile ^{13}C spectra of solid CH_3CN. Equations are derived to extend the theory beyond the adiabatic approximation.

INTRODUCTION

In this paper, we present simulations of nuclear magnetic resonance data, allowing the determination of up to 12 NMR parameters describing chemical-shift, dipole, and electric quadrupole interactions, using least-squares fits to a single (1-D) NMR spectrum. The spectra are obtained using standard magic-angle-sample spinning techniques, except that measurements are made away from the magic angle and at relatively slow spinning rates. In this context, a slow spinning rate is one which yields a spectrum with many spinning sidebands.

Magic-angle spinning (MAS) is a proven technique to obtain detailed quantitative information from high-resolution NMR measurements of solids. In ideal circumstances (high spinning speed at the magic angle), narrow NMR lines at frequencies determined by the isotropic interactions are observed, which simplifies the spectrum and increases the sensitivity compared to measurements of stationary samples. When the spinning rate is reduced, information about the chemical-shift and nuclear dipole–dipole tensors can be obtained (*1, 2*). In the case where the spin axis is not along the magic angle and the spinning rate is reduced, all the information present in the NMR spectrum from a stationary sample is present, and can, in principle, be deduced with a sensitivity improvement approaching that of a MAS measurement. Slow variable-angle sample spinning (SVASS) has been discussed by Sethi, Alderman, and Grant (*3*) and by Ding, Hu, and Ye (*4*). The situation is complicated for the case where one (or both) of the nuclei experience an electric quadrupole interaction comparable to the Zeeman interaction. An important example is ^{13}C NMR studies for carbons bonded to nitrogen (C–N) (*5*). That case is illustrated in this work using spectra of the nitrile ^{13}C in CH_3CN as an example. The results presented here are applicable to spectra for any spin-$\frac{1}{2}$ nucleus with any neighbor nucleus. For variable-angle spinning in the case where the observed nucleus experiences a quadrupole splitting see Ganapathy *et al.* (*6*) and Chen *et al.* (*7*).

The simulations are developed directly from quantum mechanical results, are an extension of previous, more limited simulations, and also include the limiting case where the sample spinning rate is zero (a stationary sample). Zilm and Grant (*8*) describe a method to calculate ^{13}C powder patterns for a stationary sample including chemical-shift anisotropy and the usual secular dipole interaction (i.e., what are usually called the A and B terms) with another nucleus. When carbon is bonded to nitrogen, it is often the case that the ^{14}N nuclear quadrupolar interaction is large enough so that the quantization axis for the nitrogen nuclear levels is not along the applied magnetic field. Since the ^{13}C ($I = \frac{1}{2}$) and ^{14}N ($S = 1$) are not quantized along the same axis, the calculation of the nuclear dipole–dipole interaction must also include terms involving the operators I_zS_x and I_zS_y (i.e., what are usually called the C and D terms) where the applied magnetic field is along the z axis. The frequency shifts due to the additional terms do not average to zero in the presence of magic-angle spinning.

The dipolar coupling between two spins, $I = \frac{1}{2}$ and $S > \frac{1}{2}$, has been described by VanderHart *et al.* (*9*), and the extra terms were used to correct a second-moment calculation for a polycrystalline sample with negligible chemical-shift anisotropy. Calculations including the chemical-shift anisotropy have been presented by Stoll *et al.* (*10*) for single crystals. Hexem *et al.* (*11*) and Naito *et al.* (*12*) each provide a detailed discussion of the effects of the ^{14}N quadrupolar

1064-1858/96 $18.00

interaction on the C–N dipole couplings as measured using magic-angle spinning. Gan and Grant (*13*) present a method to calculate lineshapes using average Hamiltonian theory, equivalent to first-order perturbation theory, valid in the fast spinning limit. That method is valid for coupled C–N spins provided the N quadrupole interaction is not too large.

Sethi *et al.* (*3*) have presented a method to calculate spectra for variable spinning speeds and angles including the case of carbon bonded to nitrogen. Their method is based on a Fourier expansion of a classical model for the motion of the ^{13}C magnetization. An infinite set of homogeneous equations describing all the sidebands is truncated to include the sidebands of importance, and a Fourier analysis of the time-dependent frequency shifts, also truncated for the case of C–N, is solved. The C–N case received only limited experimental verification. While truncation seems quite reasonable, it has yet to be formally justified. When the number of sidebands becomes large (that is, the spinning rate is slow compared to the chemical-shift anisotropy), the number of sidebands of importance increases as does the computation time. We have not used their method, but have used a straightforward computation of the lineshape similar to that described by Maricq and Waugh (*1*) and by Herzfeld and Berger (*2*), but extended by inclusion of the nitrogen quadrupole effects. As discussed below, the bulk of the computation time is devoted to diagonalizing the nitrogen Hamiltonian for different molecular orientations, and hence any computational advantages of Sethi *et al.*'s method are minor for this case. In our implementation, the lineshape for the stationary sample is obtained as a limiting case by simply setting the rotor speed to zero. In addition, the computation can be carried out for any number of individual sidebands without introducing further errors. The development below is in terms of interaction tensors; however, it could equally well be formulated using irreducible representations.

Theoretical simulations are compared to experimental measurements for acetonitrile (CH_3CN) spun near the magic angle and at spinning rates comparable to the dipolar interaction. Acetonitrile has a large chemical shift, small carbon–nitrogen internuclear distance, and hence a relatively large nuclear dipolar interaction, and the nitrogen electric quadrupole interaction is large compared to many other nitrogen-containing compounds. Hence, the limit of the slow spinning rate can be tested without the need for special equipment. In addition, isotopic enrichment with ^{15}N ($S = \frac{1}{2}$) allows a direct comparison between spectra for the same material obtained with and without a quadrupole splitting on the neighbor nucleus.

THEORY

For concreteness, the theory below is developed specifically for carbon bonded to nitrogen. The theory is readily extended to any spin-$\frac{1}{2}$ nucleus with any neighbor. The theory is developed for a general spin axis and the spinning rate can be any value between zero and a maximum determined by the quadrupole splitting (if any) of the neighbor nucleus. For ^{13}C bonded to nitrogen, all spinning rates currently available can be used.

Stationary Samples

The Hamiltonian for an isolated C–N pair is taken to be

$$H = -\gamma_I\hbar\mathbf{H}\cdot(1+\boldsymbol{\sigma})\cdot\mathbf{I} - \gamma_S\hbar\mathbf{H}\cdot\mathbf{S} + \mathbf{S}\cdot\mathsf{Q}\cdot\mathbf{S} + \mathbf{I}\cdot\mathsf{D}\cdot\mathbf{S}, \quad [1]$$

where $\mathbf{H}$ is the applied magnetic field, 1 is a unit tensor, $\boldsymbol{\sigma}$ is the carbon chemical-shift tensor, and γ_I and γ_S are the gyromagnetic ratios for the carbon and nitrogen respectively, Q is the electric quadrupole tensor, and D is the tensor for the dipole interaction. Note that with this definition, a positive chemical shift causes an increase in the resonant frequency for a fixed magnetic field. The chemical shift for the nitrogen is ignored since it will prove immaterial when computing the ^{13}C signal. The dipolar interaction is small and will be treated using perturbation theory. After diagonalizing the carbon Zeeman Hamiltonian and the nitrogen Zeeman plus quadrupolar Hamiltonians separately, a product wavefunction, expressed using eigenstates of I_z and S_z respectively, is obtained,

$$|\psi_C\rangle|\psi_N\rangle = (\beta_+|+\tfrac{1}{2}\rangle + \beta_-|-\tfrac{1}{2}\rangle) \times (\alpha_{+1}|\psi_{+1}\rangle + \alpha_0|\psi_0\rangle + \alpha_{-1}|\psi_{-1}\rangle), \quad [2]$$

where the nitrogen wavefunction is expressed in terms of eigenfunctions, $|\psi_j\rangle$, of the nitrogen Zeeman plus quadrupolar Hamiltonians,

$$|\psi_j\rangle = a_{j,+1}|+1\rangle + a_{j,0}|0\rangle + a_{j,-1}|-1\rangle, \quad [3]$$

which have energy E_j. More generally, six coefficients are needed to describe this wavefunction: however, the use of five is equivalent to assuming a random phase between the carbon and nitrogen wavefunctions and will have no consequence in what follows. Taking $\mathbf{H}$ along the z axis with magnitude H_o, and ignoring the small off-diagonal terms due to the carbon chemical-shift tensor, the eigenstates for the carbon correspond to $(\beta_+, \beta_-) = (1, 0)$ and $(0, 1)$ with energies $-\gamma_C\hbar H_o\,(1+\sigma_{zz})/2$ and $+\gamma_C\hbar H_o\,(1+\sigma_{zz})/2$, respectively.

The first-order corrections to the energy due to the dipolar term for the (approximate) eigenfunctions, $|\pm\tfrac{1}{2}\rangle|\psi_j\rangle$ are given by

$$\hbar\omega^D_{\pm,j} = \pm\tfrac{1}{2}\sum_{k=x,y,z} D_{zk}\langle\psi_j|\mathbf{S}_k|\psi_j\rangle, \quad [4]$$

where once again the terms involving $\mathbf{I}_x$ and $\mathbf{I}_y$ are small compared to the Zeeman Hamiltonian and are dropped.

If the signal is detected with a coil with its axis along the x direction, the contribution to the signal from this isolated C–N pair will be proportional to the real part of the time derivative of $\langle I_+ \rangle$, where

$$\langle I_+ \rangle = \beta_+^* \beta_- \sum_{j=-1,0,+1} \alpha_j^* \alpha_j \exp[-i\gamma_C H_o(1 + \sigma_{zz})t] \times \exp[i\omega_j^D t] \quad [5]$$

and $\omega_j^D = \omega_{+,j}^D - \omega_{-,j}^D$.

Assuming intermolecular interactions are negligible, the total signal will be the sum of similar terms. In the high-temperature (and random-phase) approximation(s), $\alpha_j^* \alpha_j$ is replaced by $\langle \alpha_j^* \alpha_j \rangle$ which to a very good approximation will be independent of j. Assuming $\langle \beta_+^* \beta_- \rangle$ is made to be nonzero (by an RF pulse), then the signal has three frequency components, of equal magnitude.

For a powder sample, contributions for all orientations of the magnetic field relative to the C–N pair must be added together. To do this, it is convenient to define a molecular reference frame and a laboratory reference frame. In these calculations, we use the principal axes of the carbon chemical-shift tensor, $\boldsymbol{\sigma}$, to define the molecular reference frame. The chemical-shift, dipolar, and quadrupolar tensors in their principal axes systems are designated $\boldsymbol{\sigma}_o$, D_o, and Q_o respectively. The diagonal elements of D_o and Q_o are given by

$$D_{xx} = 1,\ D_{yy} = 1,\ D_{zz} = -2;\ \text{in units of } \gamma_C \gamma_N \hbar^2 / r_{CN}^3,$$

where r_{CN} is the carbon–nitrogen distance, and

$$Q_{xx} = -(1 - \eta),\ Q_{yy} = -(1 + \eta),\ Q_{zz} = 2;$$
$$\text{in units of } e^2 qQ/4\hbar.$$

Note that J coupling is assumed to be small and is neglected in this work.

Defining the rotations R_D, R_Q, and $\mathsf{R}_{\boldsymbol{\sigma}}$, where R_D rotates from the dipolar principal axes to the chemical-shift principal axes, R_Q rotates from the quadrupolar principal axes to the chemical-shift axes, and $\mathsf{R}_{\boldsymbol{\sigma}}$ rotates from the chemical-shift principal axes to the laboratory reference frame, then

$$\mathsf{D} = \mathsf{R}_{\boldsymbol{\sigma}} \mathsf{R}_D \mathsf{D}_o \mathsf{R}_D^T \mathbf{R}_{\boldsymbol{\sigma}}^T$$
$$\mathsf{Q} = \mathsf{R}_{\boldsymbol{\sigma}} \mathsf{R}_Q \mathsf{Q}_o \mathsf{R}_Q^T \mathsf{R}_{\boldsymbol{\sigma}}^T \quad [6]$$

and

$$\boldsymbol{\sigma} = \mathsf{R}_{\boldsymbol{\sigma}} \boldsymbol{\sigma}_o \mathsf{R}_{\boldsymbol{\sigma}}^T$$

in the Hamiltonian (Eq. [1]) when the angular momentum operators are expressed in the laboratory reference frame. The rotations R_D and R_Q are fixed by the molecular geometry. The rotation $\mathsf{R}_{\boldsymbol{\sigma}}$ can be described using the usual two polar angles, θ and ϕ, which orient the magnetic field with respect to the chemical-shift principal axes.

Since the method described by Zilm and Grant (*8*) is not applicable unless the quadrupole contribution is negligible, a brute force technique was employed to do the powder averages. For equal increments of $\cos(\theta)$ between 1 and -1, and of ϕ between 0 and 2π, the tensors are rotated into the lab frame, the nitrogen Hamiltonian is diagonalized to get $\{|\psi_j\rangle\}$, the frequencies of the three contributions are calculated and combined with σ_{zz}, and a histogram of the responses verses frequency is created. Broadening is added after the histogram is created to smooth and to better represent the measured spectrum. Although not implemented here, the ideas for improved sampling in powder spectrum calculations presented by Alderman, Solum and Grant (*14*) might be useful to speed up the calculations.

Spinning Samples

With sample spinning at a frequency ω_r about an axis which makes an angle β with the magnetic field, the tensors in Eq. [1] can be written

$$\mathsf{D} = \mathsf{R}_{-\beta} \mathsf{R}_\phi(t) \mathsf{R}_\beta \mathsf{R}_\sigma \mathsf{R}_D \mathsf{D}_o \mathsf{R}_D^T \mathbf{R}_{\boldsymbol{\sigma}}^T \mathsf{R}_{\boldsymbol{\beta}}^T \mathsf{R}_{\boldsymbol{\phi}}^T(t) \mathsf{R}_{-\beta}^T$$
$$\mathsf{Q} = \mathsf{R}_{-\beta} \mathsf{R}_{\boldsymbol{\phi}}(t) \mathsf{R}_\beta \mathsf{R}_{\boldsymbol{\sigma}} \mathsf{R}_Q \mathsf{Q}_o \mathsf{R}_Q^T \mathbf{R}_{\boldsymbol{\sigma}}^T \mathsf{R}_{\boldsymbol{\beta}}^T \mathsf{R}_{\boldsymbol{\phi}}^T(t) \mathsf{R}_{-\boldsymbol{\beta}}^T \quad [7]$$

and

$$\boldsymbol{\sigma} = \mathsf{R}_{-\beta} \mathsf{R}_\phi(t) \mathsf{R}_\beta \mathsf{R}_{\boldsymbol{\sigma}} \boldsymbol{\sigma}_o \mathsf{R}_{\boldsymbol{\sigma}}^T \mathsf{R}_\beta^T \mathsf{R}_\phi^T(t) \mathsf{R}_{-\beta}^T,$$

where R_β rotates from the laboratory frame to the rotation axis, and $\mathsf{R}_\phi(t)$ rotates about the spinner axis by $\phi = \omega_r t$. We will be most interested in the case where β is near the magic angle (54.735°). All the tensors are now time dependent due to the sample spinning.

Zilm and Grant (*8*) show that, in the absence of the electric quadrupole effects, the ^{13}C frequency shifts can be combined to get an angular dependence identical to that of an anisotropic chemical shift. Hence, under MAS conditions, those terms which do not depend on the presence of the electric quadrupole effects will average to a single frequency. Under conditions of magic-angle spinning at rates in the range 1 to 10 kHz, one cannot expect the nitrogen quadrupole interaction, with frequencies in the 1 MHz range, to average, even though the effect on the ^{13}C resonance will be shifts smaller than 1 kHz. If angles other than the magic angle are used, none of the interactions will average to a single frequency and a powder lineshape results.

To model this situation, we start with nitrogen wavefunctions expressed in terms of a time-dependent basis set. That is, the nitrogen wavefunction is written as

$$|\psi_N(t)\rangle = \sum_{j=-1,0,+1} \alpha_j(t) |\psi_j(t)\rangle \exp[-i\Delta_j(t)], \quad [8]$$

where at any specific time t, the orthonormal basis functions $|\psi_j\rangle$ diagonalize the nitrogen Zeeman and quadrupolar interactions

$$H_N(t)|\psi_j(t)\rangle = E_j(t)|\psi_j(t)\rangle \quad [9]$$

and

$$\Delta_j(t) = \int_0^t dt\, E_j(t)/\hbar. \quad [10]$$

This wavefunction is quite general; however, it is hoped that the time dependence of $\{\alpha_j(t)\}$ is small.

Following the same procedure as above, except using the wavefunction in Eq. [8], Eq. [5] becomes

$$\langle I_+\rangle = \beta_+^*\beta_- \sum_{j=-1,0,+1} \alpha_j^*(t)\alpha_j(t)\exp[-i\gamma_C H_o t - i\Sigma_{zz}] \times \exp[i\,\Omega_j], \quad [11]$$

where

$$\Sigma_{zz}(t) = \gamma_C H_o \int_0^t dt\, \sigma_{zz}(t) \quad [12]$$

and

$$\Omega_j(t) = \int_0^t dt\, \omega_j^D(t).$$

The problem now is to find $\{\alpha_j(t)\}$ and to take an appropriate ensemble average.

In principle, $\{\alpha_j(t)\}$ can be determined by substituting Eq. [8] into the Schrödinger equation

$$H_N\,|\psi_N(t)\rangle = -\frac{\hbar}{i}\frac{\partial}{\partial t}\,|\psi_N(t)\rangle \quad [13]$$

to get

$$\frac{\partial\alpha_k}{\partial t} + \sum_{j=-1,0,+1} \alpha_j\langle\psi_k|\left(\frac{\partial}{\partial t}\,|\psi_j\rangle\right) \times \exp[-i(\Delta_j - \Delta_k)] = 0. \quad [14]$$

Up to this point, no additional approximations have been added to those used for the static case. Rather than solve this differential equation, we seek an approximate solution. If we assume $\{\alpha_j(0)\}$ are known, then a short time later, $\Delta t \ll 1/\omega_r$, we get an approximate solution

$$[\alpha_k(\Delta t) - \alpha_k(0)]/\Delta t \approx -\sum_{j=-1,0,+1} \alpha_j(0)\langle\psi_k|\left(\frac{\partial}{\partial t}\,|\psi_j\rangle\right) \times \frac{\{\exp[-i(E_j(0) - E_k(0))\Delta t/\hbar] - 1\}}{-i[E_j(0) - E_k(0)]\Delta t/\hbar} \quad [15]$$

valid if $\alpha_k(t)$ does not vary too much during the time Δt. Since we are interested in the behavior at times of order $1/\omega_r$ and $|E_j - E_k| \gg \hbar\omega_r$ for $j \neq k$, we can use the fact the denominator is large and/or stroboscopic sampling to get

$$\frac{\partial\alpha_k}{\partial t} = -\alpha_k(t)\langle\psi_k|\left(\frac{\partial}{\partial t}\,|\psi_k\rangle\right). \quad [16]$$

If the effects of the electric-field gradient (EFG) can be described using perturbation theory, the right-hand side can be calculated using

$$\langle\psi_k|\left(\frac{\partial}{\partial\omega_r t}\,|\psi_k\rangle\right) = \sum_{m\neq k} \frac{i}{\gamma H_o(k-m)}\,\langle m|H_Q|k\rangle\langle m|[H_Q, \mathbf{I}_r]|k\rangle \quad [17]$$

where H_Q is the time-dependent electric quadrupole portion of the nitrogen Hamiltonian, $\mathbf{S}\cdot\mathbf{Q}\cdot\mathbf{S}$, (Eqs. [1] and [7]), and $\mathbf{I}_r$ is the angular momentum operator along the spinning axis. The right side of Eq. [17] is second order in the perturbation. Thus, the time evolution of $\alpha_k\alpha_k^*$ will be second order in the perturbation. For the situations where the nitrogen wavefunctions are described reasonably well using first-order perturbation theory, the time evolution gives a small contribution and one can take $\alpha_k\alpha_k^*$ to be time independent. With this approximation, the equations describing the NMR signal are the same as those derived using the adiabatic approximation (*11, 12*). It should be noted that, in any event, the method (as well as those presented by others) may fail to produce correct results if the nitrogen energy levels cross (so $|E_j - E_k| \approx \hbar\omega_r$ for $j \neq k$) as the sample spins. For typical electric-field gradients observed for ^{14}N ($e^2qQ = 1$ to 4 MHz), this will not be an issue except for magnetic fields below about 1 T. In contrast, if the neighbor were Cl, the level crossings may occur for fields below about 9 T. The term $\langle\psi_k|\,[(\partial/\partial t)\psi_k\rangle]$ in Eq. [16] will be periodic with frequency ω_r about an average of zero. By expanding that term in a Fourier series, it is straightforward to show that $\alpha_k(t)\alpha_k^*(t)$ can be written in the form

$$\alpha_k(t)\alpha_k^*(t) = \alpha_k(0)\alpha_k^*(0)\exp[\zeta(t) - \zeta(0)], \quad [18]$$

where $\zeta(t)$ is a real function of time, periodic with frequency ω_r. That is, there will be a small amount of amplitude modulation of the NMR signal in addition to the frequency modulation shown in Eq. [14].

Up to this point, the discussion has been for an isolated C–N pair which has a particular initial orientation with respect to the magnetic field. We now wish to consider the

ensemble average of all such pairs which have the same orientation. To do this, we make the assumption that at any starting point ($t = 0$) all possible wavefunctions are present with equal probability. That is, we use the usual high-temperature, random-phase approximation. Hence, within our time-independent approximation, $\langle \alpha_j^*(0)\alpha_j(0)\rangle = \langle \alpha_k^*(0)\alpha_k(0)\rangle$. Alternatively, we can define the initial condition in terms of eigenfunctions of the time-averaged Hamiltonian, again assuming the high-temperature, random-phase approximation. The result in either case is the same.

We write the remaining real-valued functions of time, σ_{zz}, and ω_j^{D}, using

$$\omega_\sigma(t) = \gamma_{\mathrm{C}} H_{\mathrm{o}} \sigma_{zz}(t) = \omega_{\mathrm{o}} + \omega_{\mathrm{a}}(t)$$
$$\omega_j^{\mathrm{D}}(t) = \omega_{j\mathrm{o}}^{\mathrm{D}} + \omega_{j\mathrm{a}}^{\mathrm{D}}(t), \qquad [19]$$

where ω_{o} and $\omega_{j\mathrm{o}}^{\mathrm{D}}$ are the time average values, and $\omega_{\mathrm{a}}(t)$ and $\omega_{j\mathrm{a}}^{\mathrm{D}}(t)$ will be periodic with rotation frequency ω_{r}, the spinning frequency. Defining a function $\xi_j(t)$ such that

$$\frac{d\xi_j}{dt} = \omega_{j\mathrm{a}}^{\mathrm{D}}(t) - \omega_{\mathrm{a}}(t),$$

and suppressing constant terms, we find that

$$\langle I_+ \rangle = \sum_{j=-1,0,+1} \exp[-i(\omega_{\mathrm{o}} - \omega_{j\mathrm{o}}^{\mathrm{D}})t] \times \exp\{i[\xi_j(t) - \xi_j(0)] + [\zeta_j(t) - \zeta_j(0)]\}. \qquad [20]$$

The frequency modulation (the imaginary terms in the second exponential) has a significant impact on the observed lineshape if the spinning frequency is not large compared to the chemical shift anisotropy and/or the dipole interaction.

Numerical computation of lineshapes using Eq. [20] was done in a manner similar to the calculations for the stationary samples except that the powder average was done using the spinner axis rather than along the direction of the magnetic field. That is, in Eq. [7], $\mathsf{R}_\beta\mathsf{R}_\sigma$ is replaced by a single rotation directly to the spinner axis, $\mathsf{R}(\alpha, \beta, \gamma)$, and $\mathsf{R}_\phi(t)\,\mathsf{R}(\alpha, \beta, \gamma) = \mathsf{R}(\alpha, \beta, \gamma + \omega_{\mathrm{r}}t)$. The chemical shift and dipole shifts sampled for one rotation of the spinner are used, and the intensity of each contribution is modified by the second exponential in Eq. [20], as discussed below. To obtain simulations in a reasonable amount of time, the small-amplitude modulation is neglected.

Since we are interested in the nth order sideband lineshape, a Fourier transform of the second exponential in Eq. [20] is needed. We use a simplified version of the method described by Mehring (*15*). An unnecessary numerical average over γ can be avoided if that average is computed as follows. Recognizing that γ is equivalent to a time $t_{\mathrm{o}} = \gamma/\omega_{\mathrm{r}}$, the Fourier transform of the frequency modulating terms is

$$\int_0^{2\pi/\omega_{\mathrm{r}}} dt\, \exp\{i[\xi(t + t_{\mathrm{o}}) - \xi(t_{\mathrm{o}}) - n\omega_{\mathrm{r}}t]\}$$
$$= \exp\{-i[\xi(t_{\mathrm{o}}) - n\omega_{\mathrm{r}}t_{\mathrm{o}}]\} \times \int_0^{2\pi/\omega_{\mathrm{r}}} dt'\, \exp\{i[\xi(t') - n\omega_{\mathrm{r}}t']\}$$
$$= \exp\{-i[\xi(t_{\mathrm{o}}) - n\omega_{\mathrm{r}}t_{\mathrm{o}}]\}\, F_n = G_n, \qquad [21]$$

where the fact that $\xi(t)$ is periodic has been used. After the average over γ (e.g., t_{o}), the intensity is $F_nF_n^* = G_nG_n^*$. To implement this numerically, ω_σ and ω_j^{D} are accumulated as the angle γ is incremented by 2π in equal steps. The number of steps must be large enough to avoid Nyquist folding. After subtracting the average values, the integrals (Eq. [12]) are computed and an array containing the exponentials is formed. The array is Fourier transformed for the sidebands of interest and each element is squared. This results in the computation of $|G_n|^2$. The intensity is then placed into a lineshape histogram at the position corresponding to the frequency $\omega_{\mathrm{o}} - \omega_{j\mathrm{o}}^{\mathrm{D}} - n\omega_{\mathrm{r}}$. If many sidebands are desired, it is convenient to choose the number of steps to be a power of two so that a fast Fourier transform can be applied. Broadening is added to smooth the spectrum using a simple convolution with a single broadening function. Relaxation effects are not included except to the extent they are modeled by the broadening. The same theory is used to compute lineshapes for carbon bonded to ^{15}N ($S = \frac{1}{2}$), except that the terms involving $\langle S_x\rangle$ and $\langle S_y\rangle$ are excluded and the diagonalization of the nitrogen Hamiltonian is unnecessary.

Changes in the spinning rate during signal averaging can lead to significant changes in the observed lineshape if sharp features are present. Slow changes in the spinning rate during signal averaging were simulated using a square distribution for ω_{r} about its average value when placing the intensity into the histogram. This approximate treatment will only be valid when the spinning rate changes are small.

We typically use a minimum of 32 values of γ and a fast Fourier transform (*16*), allowing up to 15 sidebands on either side of the zeroth-order spectrum to be computed. For slower speeds, the number of samples is increased. Simulations have been performed with up to 512 sidebands without difficulty. To speed the calculation, the diagonalization of the nitrogen Hamiltonian is done using the results of exact equations (*17*). There are a small number of special cases where that routine fails and they are avoided. In any event, they would be rare and the contribution to the resultant spectrum would be negligible. Simple timing measurements show that about one-half of the time is spent diagonalizing the nitrogen Hamiltonian to find the nitrogen wavefunctions and less than one-tenth of the time is used to compute the

intensities. The Euler angles defined by Edmonds (*18*) were used. A look-up table was computed for the rotation operators describing the sample spinning as a trade-off between speed and memory use. Calculations were done using a desktop computer with a 486DX/4-100 MHz processor. With that computer, a lineshape calculation takes a few seconds for completely axial interactions to several minutes for more complicated situations.

Unweighted-least-squares fits were performed using a modified version of the Levenberg–Marquardt method. That method is described by Press *et al.* (*19*). Derivatives with respect to the parameters were calculated numerically and the number of function calls was kept to a minimum (one call per parameter per iteration). In addition to 12 adjustable physical parameters (3 describing the chemical shift, 3 describing the dipole interaction, 5 describing the EFG, and 1 describing the broadening), we have also included 7 adjustable experimental parameters (an overall amplitude, the angle of the spin axis, the spinner rate and stability, and up to 3 parameters to describe a parabolic baseline). Fits using all 19 adjustable parameters are quite time consuming and in some cases have produced unreliable results, and an appropriate subset is used in each case. Least-squares fits can take anywhere from a few minutes to over an hour, depending on the number of adjustable parameters and the quality of the initial guesses for those parameters.

As a side note, a measurement of the ^{13}C NMR signal in the presence of nitrogen can be used to determine the diagonal terms of the nitrogen density matrix. Since the C–N interaction is weak, and in most cases relaxation processes are very slow, transitions between the N energy levels during the time scale of the measurement are negligible. The ensemble average (Eq. [20]) would be unchanged if one were to assume that the nitrogen wavefunction ''collapsed'' due to this measurement process. If a collapse occurred, each nitrogen would only be observed in one of its eigenstates, rather than a linear combination of eigenstates. Should a measurement of a single isolated C–N pair be possible, the individual measured responses (Eq. [11]) would be very different if the wavefunction collapsed due to the measurement process than if a wavefunction remained a linear combination of the eigenstates during the time scale of the measurement.

COMPARISON OF THEORY AND EXPERIMENT

Solid CH_3CN was chosen because the chemical-shift, C–N dipole interaction, and N electric quadrupole coupling allow for a direct comparison between theory and experiment without the need for special equipment and/or techniques. In fact, it is quite difficult to achieve the fast-spinning limit for this compound.

The experimental spectra for CH_3CN were measured as previously described (*20, 21*), using proton decoupling with the addition of cross polarization for natural-abundance ^{13}C samples, a homebuilt spectrometer at a field of 3.5 T (37.84 MHz for ^{13}C), and a Doty (*22*) (DSI-574) probe. Spectra are referenced to TMS using adamantane as a secondary reference. Calibration of the stator angle was done using the ^{79}Br resonance of KBr.

The nitrile carbon of solid acetonitrile (CH_3CN) has a chemical-shift anisotropy of over 300 ppm (approx. 10 kHz at 3.5 T), making the limit of rapid sample spinning quite difficult to achieve. The short C≡N bond length results in a relatively large dipolar interaction ($\gamma_C \gamma_N \hbar^2 / r_{CN}^3 \approx 35$ ppm or about 1 kHz at 3.5 T). The effects of the ^{14}N (100% natural abundance) electric-quadrupole-field splitting [e^2qQ = 3.738 MHz (*23*)] on the CH_3CN ^{13}C spectra will be angular-dependent frequency shifts of about ±10 ppm at 3.5 T. Spinning rates as low as 570 Hz (less than 1/10th of the linewidth, and about 1/2 of the dipole coupling) were used. When the spinning rate is this small, and the chemical-shift anisotropy so large, a deviation of 1° or so from the magic angle is all that is necessary to obtain significant results. While there is no single scaling factor, comparable spectra for typical C–N-containing materials, such as for the α carbon of L-alanine, which has a smaller chemical-shift anisotropy (*24*), smaller electric quadrupole splittings, and a larger C–N distance (*11*), would be acquired with a spinning rate of about 100 Hz.

CH_3CN has two solid phases, a higher-temperature α phase stable between 217 and 229 K and a β phase stable below 217 K with a slow conversion between the two phases at the transition. The measurements presented here are for samples slowly cooled through the α phase and the samples will be predominantly β phase (*25*). In any event, no difference could be observed in the NMR spectra of the α and β phases (*20*). The CH_3CN molecule is linear and X-ray (*26*) and neutron-diffraction (*27*) studies are consistent with a linear molecule within the solid. Hence, one can expect the nitrile carbon NMR parameters to represent an axial environment.

Figure 1 shows ^{13}C NMR spectra and theoretical simulations from least-squares fits for CH_3CN enriched to 99% ^{15}N (Cambridge Isotope Labs) spun about the magic angle, β_M, and at $\beta_M - 1.8°$. A large peak near 0 ppm, from the methyl carbon, was not included in the simulations. The simulations shown in all figures have had baseline effects removed. Since ^{15}N has $S = \frac{1}{2}$, the effects of the N electric quadrupole field will be unobservable. The spectrum in Fig. 1a consists of about nine usable sharp features (only eight are shown). The overall amplitude of the spectrum can be set using one of the lines, and the linewidth of the spectrum is set by the data near that line. The isotropic chemical shift is easily determined using the zero-order sideband (near 122 ppm). Thus, only the relative amplitudes of eight of these lines need to be specified to model the entire lineshape. That is, there are eight values to be fitted. A general fit would include two additional chemical-shift parameters, an internuclear

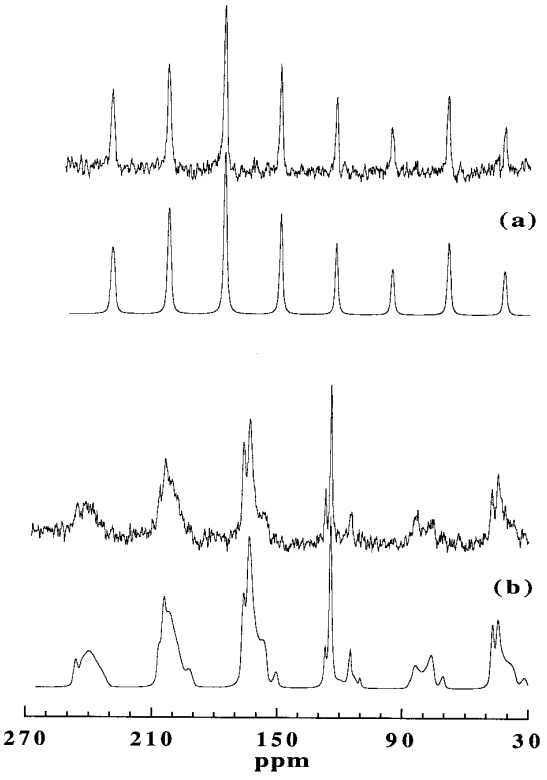

FIG. 1. Experimental ^{13}C NMR proton-decoupled sample-spinning spectrum and simulations for ^{15}N-enriched $CH_3C^{15}N$ at (a) the magic angle and (b) the magic angle minus 1.8°, at a spinning frequency of 1010 Hz. The methyl carbon signal is near 0 ppm and was not included in the simulation. The parameters used for the simulations are a result of unweighted-least-squares fits. Values are discussed in the text.

distance, two angles describing the orientation of the internuclear vector, and for very narrow features, even a very small spin-rate instability can have an appreciable effect and must be included. In addition, changes in the rotation angle by as little as 0.2° can change the relative intensities, and hence, the rotation angle becomes a parameter if it is not known to better than 0.2°. Thus, one has as many as eight parameters to be determined from the eight values. Statistical estimates from such a fit to the data in Fig. 1 yield, for example, an internuclear distance, $R = 1.15 \pm 0.08$ Å. The spectrum in Fig. 1b contains more information and fits yield an internuclear distance of $R = 1.14 \pm 0.03$ Å.

Figures 2 and 3 show ^{13}C NMR spectra and theoretical simulations for ^{13}C-enriched, solid $CH_3{}^{13}CN$ near 140 K for various spinning rates and at various angles near the magic angle. These spectra are rich with structure, and hence, one can hope to extract more information from the data. In order to compare to the ^{15}N-enriched sample, fits were done restricting the nitrogen EFG to its known value measured at 77 K [$e^2qQ = -3.738$ MHz and nearly axial (*23*), where the minus sign is easily determined from these measurements (*5, 11*)] and further restricting the EFG principal axes to be coincident with the chemical-shift principal axes. Lorentzian broadening was used. Individual fits to these spectra yield consistent values of $R = 1.180 \pm .010$ Å where the error expressed here well represents both the statistically estimated error for each individual fit as well as the variation from one fit to another. The chemical-shift anisotropy, $\Delta\sigma$ [$\Delta\sigma \equiv \sigma_{zz} - (\sigma_{yy} + \sigma_{xx})/2$], from the fits was -311 ± 2 ppm. Restricting the chemical shift to be axial, the EFG and dipolar principal axes to be along the chemical-shift principal axes, but allowing the magnitude of the EFG to vary, gave $R = 1.160 \pm 0.010$ Å and $e^2qQ = -3.55 \pm 0.16$ MHz. The latter fits had only a slightly reduced value of χ^2, though in several cases the relative intensities of some of the sharper features better matched the data. Although weighted fits were not pursued as part of this work, this result suggests that adding extra weight to sharper spectral features may be a good strategy for obtaining fits to these, or similar, spectra.

Note that in the fast-spinning limit, the ^{13}C spectrum will consist of two closely spaced powder patterns with an inten-

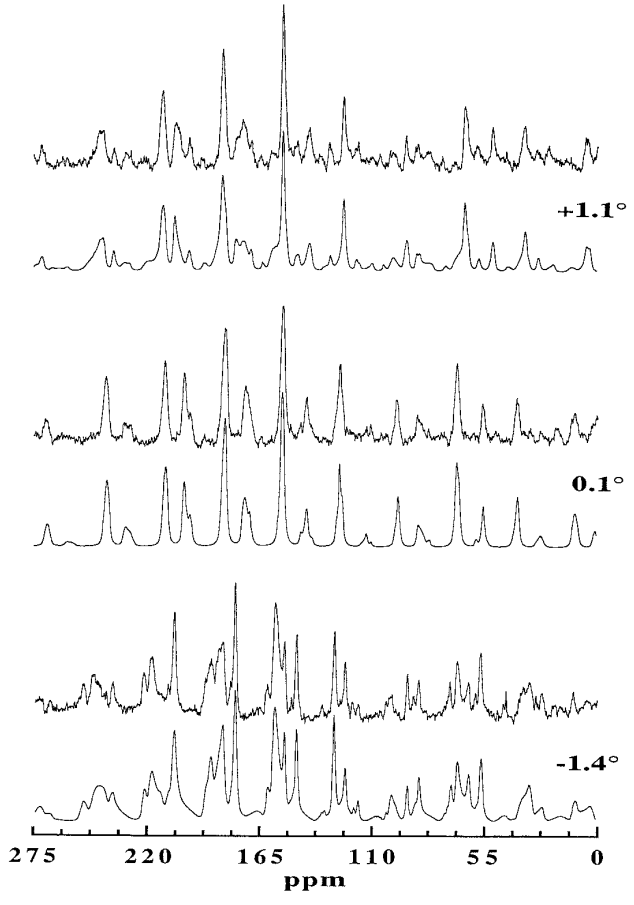

FIG. 2. Experimental ^{13}C proton-decoupled, sample-spinning spectra and simulations for ^{13}C-enriched $CH_3{}^{13}CN$ at 140 K, spinning at 1100 Hz for three offsets from the magic angle. The parameters used for the simulations are a result of unweighted-least-squares fits. Values are discussed in the text.

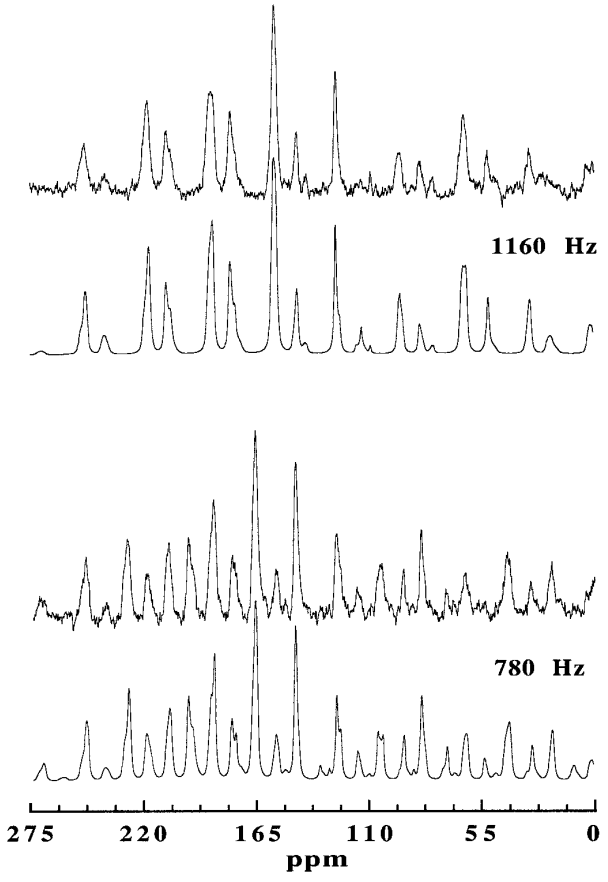

FIG. 3. Experimental ^{13}C proton-decoupled, sample-spinning spectra and simulations for ^{13}C-enriched $CH_3{}^{13}CN$ at 180 K, and at the magic angle for different spinning rates. Spectra at spinning rates of 1160 and 920 Hz (not shown) were measured at both 140 K and 180 K and no difference could be observed. The parameters used for the simulations are a result of unweighted-least-squares fits. Values are discussed in the text.

sity ratio of 2:1 corresponding to the nitrogen $S_z = \pm 1$ and 0 levels, respectively (*3, 5, 11*). At the spinning rates used here, the zero order sideband is spread out between about 115 and 130 ppm, and the intensity associated with $S_z = 0$ (near 115 to 118 ppm) is greatly reduced in intensity compared to the intensity associated with $S_z = \pm 1$—so much so that it is barely visible. This effect is illustrated in Fig. 4. Note also that in addition to a change in the 2:1 intensity ratio, there is an apparent change in the splitting between the lines at lower spinning rates.

The parameters which were determined most precisely by the fitting procedure (if allowed to vary) are the overall amplitude ($\pm 0.2\%$), the baseline ($\pm 0.02\%$ of full scale), the spinning angle ($\pm 0.03°$), the spin rate (± 0.1 Hz), the FWHM of the broadening function ($\pm 1\%$), and the isotropic chemical shift (± 0.05 ppm). The values least well determined were the Euler angles describing the orientation of the nitrogen EFG relative to the chemical-shift principal axes where variations of 10° to 20° from fit to fit were common.

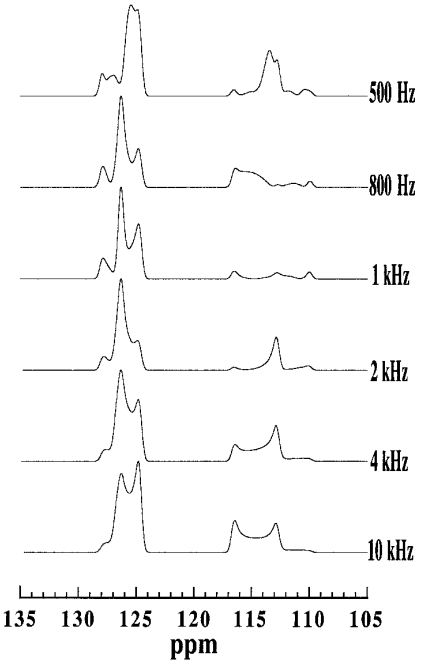

FIG. 4. Simulations of the zero-order sideband for CH_3CN spun at the magic angle for various spinning rates.

Values for other parameters are given above. The precision for determining *R* is eight times better using the data in Fig. 2 or 3 than using the data in Fig. 1a. Figure 5 shows the ^{13}C NMR spectra for a stationary CH_3CN sample along with a best-fit simulation. This sample was enriched to 99% ^{13}C at the nitrile site in order to clearly see the elements of the

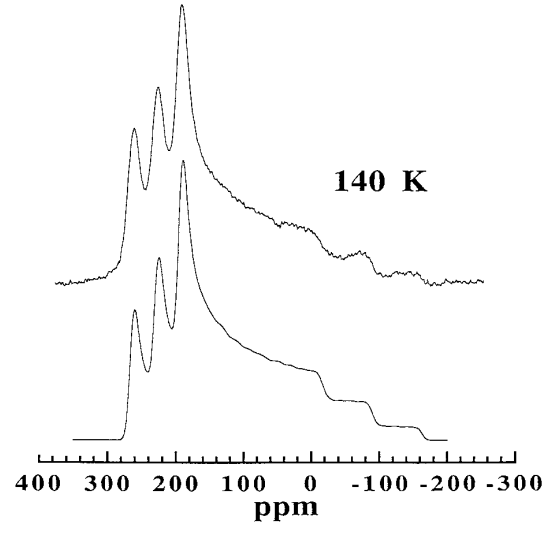

FIG. 5. Experimental ^{13}C proton-decoupled spectra and simulation for ^{13}C-enriched $CH_3{}^{13}CN$, for a stationary sample at 140 K obtained using Hahn echoes. The parameters used for the simulation are a result of unweighted-least-squares fits. Values are discussed in the text.

chemical-shift tensor without interference from the methyl carbon. The simulation is a result of a least-squares fit with the same restrictions as above. The value of R_{CN} which resulted was 1.165 ± 0.005 Å. Gaussian broadening was used. The chemical-shift anisotropy which best fitted the data was $\Delta\sigma = -318 \pm 2$ ppm, slightly larger than the values obtained from the spinning spectra. The difference between these $\Delta\sigma$ values is outside the error estimates and simulations for a stationary sample with the value −311 ppm clearly show that this value is too small to match the static spectrum. The origin of this difference is unknown, but may be due to the restrictions placed on some of the parameters during the fits or possibly to the neglect of the amplitude-modulating terms (e.g., the use of the adiabatic approximation). The effects of the nitrogen electric quadrupole interaction on the static spectrum are small (shifts of ±9 ppm), and thus, as previously noted (*28*), one cannot expect to be able to extract accurate values for e^2qQ from the static spectrum.

Additional simulations of both the static and spinning data show that $\eta_{CS} = (\sigma_{yy} - \sigma_{xx})/(\sigma_{zz} - \sigma)$, where σ is the isotropic shift, is given by $\eta_{CS} < 0.07$, also $\eta_Q < 0.1$, and the angle θ between the chemical-shift z axis and the internuclear vector is less than 10°.

CONCLUSION

Simulations of spectra for a spin-$\frac{1}{2}$ nucleus with an unlike neighbor for the general case of slow spinning speeds and off-angle spinning can be used to fit experimental data to retrieve chemical-shift parameters, internuclear bond distances, and for a quadrupolar neighbor, the electric field gradient at the neighbor site. The case of CH_3CN using ^{13}C CP-MAS NMR (proton-decoupled) spectra is presented in detail. The precision of values obtained from multiparameter fits is comparable with values obtained using a static spectrum with the exception of the ^{14}N EFG. The ^{14}N EFG is obtained much more precisely using the slow, variable-angle sample-spinning (SVASS) data. The carbon–nitrogen internuclear distance was determined more precisely using natural-abundance samples measured at slower speeds and off the magic angle than by using ^{15}N-enriched material spun at the magic angle.

ACKNOWLEDGMENTS

This work was supported in part by the U.S. National Science Foundation Grants DMR-9308168, DMR-8819885, and CTS-9403909.

REFERENCES

1. M. M. Maricq and J. S. Waugh, *J. Chem. Phys.* 70, 3300 (1979).
2. J. Herzfeld and A. Berger, *J. Chem. Phys.* 73, 6021 (1980).
3. N. K. Sethi, D. W. Alderman, and D. M. Grant, *Mol. Phys.* 71, 217 (1990).
4. S. Ding, J. Hu, and C. Ye, *Solid State NMR* 1, 103 (1992).
5. R. K. Harris and A. C. Olivieri, *Prog. NMR Spectrosc.* 24, 435 (1992), and references therein.
6. S. Ganapathy, S. Schramm, and E. Oldfield, *J. Chem. Phys.* 77, 4360 (1982).
7. T. H. Chen, J. Z. Wang, H. X. Li, K. X. Wang, F. Deng, Y. R. Du, and D. T. Ding, *Chem. Phys. Lett.* 238, 82 (1995).
8. K. W. Zilm and D. M. Grant, *J. Am. Chem. Soc.* 103, 2913 (1981).
9. D. L. VanderHart, H. S. Gutowsky, and T. C. Farrar, *J. Am. Chem. Soc.* 89, 5056 (1967).
10. M. E. Stoll, R. W. Vaughan, R. B. Saillant, and T. Cole, *J. Chem. Phys.* 61, 2896 (1974).
11. J. G. Hexem, M. H. Frey, and S. J. Opella, *J. Chem. Phys.* 77, 3847 (1982).
12. A. Naito, S. Ganapathy, and C. A. McDowell, *J. Chem. Phys.* 74, 5393 (1981).
13. Z. Gan and D. M. Grant, *J. Magn. Reson.* 90, 522 (1990).
14. D. W. Alderman, M. S. Solum, and D. M. Grant, *J. Chem. Phys.* 84, 3717 (1986).
15. M. Mehring, ''Principles of High Resolution NMR in Solids,'' 2nd ed., p. 46, Springer-Verlag, Berlin/New York, 1983.
16. Cooley, Lewis, and Welch, *IEEE Trans.* E12, no. 1 (1965).
17. J. G. Hexem, Ph.D. thesis, unpublished, University of Pennsylvania, 1982.
18. A. R. Edmonds, ''Angular Momentum in Quantum Mechanics,'' p. 7, Princeton Univ. Press, Princeton, New Jersey, 1960.
19. W. H. Press, S. A. Teukolsky, W. T. Vetterling, and B. P. Flannery, ''Numerical Recipes in Fortran,'' 2nd ed., Cambridge Univ. Press, Cambridge, 1992.
20. J. Sepa, R. J. Gorte, B. H. Suits, and D. White, *Chem. Phys. Lett.* 252, 7798 (1996).
21. K. R. Carduner, M. Villa, and D. White, *Rev. Sci. Instrum.* 55, 68 (1984).
22. Doty Scientific Inc., Columbia, South Carolina 29223.
23. H. Negita, P. A. Casabella, and P. J. Bray, *J. Chem. Phys.* 32, 314 (1960).
24. C. Ye, R. Fu, J. Hu, L. Hou, and S. Ding, *Magn. Reson. Chem.* 31, 699 (1993).
25. E. L. Pace and L. J. Noe, *J. Chem. Phys.* 49, 5317 (1968).
26. M. J. Barrow, *Acta Crystallogr. B* 37, 2239 (1981).
27. O. K. Antson, K. J. Tilli, and N. H. Andersen, *Acta Crystallogr. B* 43, 296 (1987).
28. K. Eichele, M. D. Lumsden, and R. E. Wasylishen, *J. Phys. Chem.* 97, 8909 (1993).